Title
A conserved MST1/2–YAP axis mediates Hippo signaling during lung growth

Journal
Developmental Biology, 403(1)

ISSN
0012-1606

Authors
Lin, Chuwen
Yao, Erica
Chuang, Pao-Tien

Publication Date
2015-07-01

DOI
10.1016/j.ydbio.2015.04.014

Peer reviewed

HHS Public Access

Author manuscript

Dev Biol. Author manuscript; available in PMC 2016 July 01.

Published in final edited form as:

Dev Biol. 2015 July 1; 403(1): 101–113. doi:10.1016/j.ydbio.2015.04.014.

A conserved MST1/2-YAP axis mediates Hippo signaling during lung growth

Chuwen Lin, **Erica Yao**, and **Pao-Tien Chuang**

Cardiovascular Research Institute, University of California, San Francisco, CA 94158

Abstract

Hippo signaling is a critical player in controlling the growth of several tissues and organs in diverse species. The current model of Hippo signaling postulates a cascade of kinase activity initiated by the MST1/2 kinases in response to external stimuli. This leads to inactivation of the transcriptional coactivators, YAP/TAZ, due to their cytoplasmic retention and degradation that is correlated with YAP/TAZ phosphorylation. In most tissues examined, YAP plays a more dominant role than TAZ. Whether a conserved Hippo pathway is utilized during lung growth and development is unclear. In particular, the regulatory relationship between MST1/2 and YAP/TAZ in the lung remains controversial. By employing the *Shh-Cre* mouse line to efficiently inactivate genes in the lung epithelium, we show that loss of MST1/2 kinases in the epithelium can lead to neonatal lethality caused by lung defects. This is manifested by perturbation of lung epithelial cell proliferation and differentiation. These phenotypes are more severe than those produced by *Nkx2.1-Cre*, highlighting the effects of differential Cre activity on phenotypic outcomes. Importantly, expression of YAP targets is upregulated and the ratio of phospho-YAP to total YAP protein levels is reduced in *Mst1/2*-deficient lungs, all of which are consistent with a negative role of MST1/2 in controlling YAP function. This model gains further support from both *in vivo* and *in vitro* studies. Genetic removal of one allele of *Yap* or one copy of both *Yap* and *Taz* rescues neonatal lethality and lung phenotypes due to loss of *Mst1/2*. Moreover, knockdown of *Yap* in lung epithelial cell lines restores diminished alveolar marker expression caused by *Mst1/2* inactivation. These results demonstrate that MST1/2 inhibit YAP/TAZ activity and establish a conserved MST1/2-YAP axis in coordinating lung growth during development.

Keywords

Hippo Signaling; Mst1/2; Yap; Lung Development

*Correspondence should be addressed to Pao-Tien Chuang: pao-tien.chuang@ucsf.edu.

Introduction

Hippo signaling plays a central role in tissue development, regeneration and tumor development in several tissues and organs that have been examined (Varelas, 2014). In contrast, whether the Hippo pathway executes key steps of lung development and physiology and whether aberrant Hippo signaling leads to lung pathology are underexplored (Mahoney et al., 2014; Zhao et al., 2014). The available mouse Cre lines that direct lung expression (Rawlins and Perl, 2012) and conditional alleles of Hippo pathway components would enable studies to provide a more definitive answer to the role of Hippo signaling in the lung. These investigations will also elucidate the molecular mechanisms by which Hippo signaling controls various aspects of lung biology.

The basic framework of Hippo signaling has been established through extensive work in model organisms and cell-based assays (Barry and Camargo, 2013; Gumbiner and Kim, 2014; Halder and Johnson, 2011; Harvey and Hariharan, 2012; Matsui and Lai, 2013; Pan, 2010; Staley and Irvine, 2012; Yu and Guan, 2013). At the core of the current model of mammalian Hippo signaling is a kinase cascade that controls the activity of the transcriptional coactivator, YAP (Yes-associated protein) (Huang et al., 2005; Sudol, 1994; Sudol et al., 1995), to govern multiple aspects of cell physiology. In mammals, the STE20-like protein kinases, MST1/2, phosphorylate and activate the large tumor suppressor kinases, LATS1/2 (Chan et al., 2005). Active LATS phosphorylates YAP (Oka et al., 2008) and YAP phosphorylation is associated with its cytoplasmic sequestration and degradation (Zhao et al., 2010). Consequently, the transcriptional targets of YAP in the nucleus are not activated. By contrast, when MST1/2 are inactivated in response to external signals (such as low cell density), YAP becomes hypophosphorylated and it is postulated that this form of YAP is enriched in the nucleus and activates Hippo targets in conjunction primarily with the TEA domain family transcription factors, TEAD1-4 (Jacquemin et al., 1996; Ota and Sasaki, 2008; Sawada et al., 2008). This would mediate a diverse array of cellular functions such as cell proliferation, differentiation and death. In this model, loss of MST1/2 is expected to result in a relative reduction in LATS and YAP phosphorylation.

TAZ (transcriptional co-activator with PDZ-binding motif) shares homology with YAP and also functions as a transcriptional co-activator in Hippo signaling. Loss of *Taz* in mice leads to milder phenotypes than those in *Yap* knockout mice. *Yap*-deficient embryos exhibit early lethality at 9.5-10.5 *days post coitus* (*dpc*) (Morin-Kensicki et al., 2006) and conditional inactivation of *Yap* in various tissues results in defective development or homeostasis (Reginensi et al., 2013; Schlegelmilch et al., 2011; Xin et al., 2011; Zhang et al., 2010). By contrast, although some *Taz*-deficient mice die during the perinatal and postnatal period, one-fifth of *Taz* mutant mice grow to adulthood (Makita et al., 2008). The major defects in the absence of *Taz* are renal cysts and emphysematous changes in the lung (Makita et al., 2008). Thus, while *Taz* shares functional redundancy with *Yap*, YAP is the major player in mediating Hippo signaling in most tissues.

Studies in several tissues have uncovered key aspects of Hippo signaling *in vivo* but context-dependent variations in the interactions between Hippo pathway components also seem to be prevalent (Varelas, 2014). For instance, loss of *Mst1/2* in the liver results in increased YAP

protein levels and reduced YAP phosphorylation as predicted by the model of canonical Hippo signaling; unexpectedly the phosphorylation state of LATS is unaltered in the absence of *Mst1/2* (Zhou et al., 2009). Therefore, the function and interaction of Hippo pathway components in each tissue can only be revealed by dissecting the Hippo pathway in a given tissue.

While the core components of the Hippo pathway are conserved, signals that activate the Hippo pathway and targets controlled by Hippo signaling are expected to be different in diverse tissues (Varelas, 2014). In this regard, not only is the full spectrum of Hippo signaling effects on lung biology and pathology yet to be revealed, but the upstream regulators and downstream effectors of Hippo signaling in the lung are also largely unknown. A prerequisite to answering these important questions relies on establishing the function and interaction of individual Hippo pathway components in the lung. For instance, removal of *Yap* in the lung epithelium results in defective lung development (Mahoney et al., 2014), supporting an essential role of Hippo signaling in controlling lung growth. However, this issue is complicated by a recent report (Chung et al., 2013) in which the MST1/2 kinases were shown to regulate the transcription factor FOXA2 and not YAP during lung development. In this study, we employ multiple mouse Cre lines as well as lung cell lines to investigate the interactions between MST1/2 and YAP in controlling lung growth. Our findings indicate that the MST1/2-YAP axis is conserved in the lung. We surmise that variable efficiencies of the mouse Cre lines contribute to the seeming discrepancy in the regulatory relationship between MST1/2 and YAP in the lung.

Materials and methods

Animal husbandry

Shh-Cre [B6.Cg-*Shh*$^{tm1(EGFP/cre)Cjt}$/J] and *Nkx2.1-Cre* [C57BL/6J-Tg (Nkx2-1-cre)2Sand/J] mice were obtained from Jackson Laboratory. *Mst1* null and *Mst2* floxed alleles were given to us by Dr. Yingzi Yang. *Yap* and *Taz* floxed alleles were provided by Dr. Eric Olson. The Institutional Animal Care and Use Committee at the University of California, San Francisco, approved all experiments performed in this study.

Histology and immunohistochemistry

Mouse embryos or adult mice were harvested at indicated time points and the embryos or lungs were fixed in 4% paraformaldehyde (PFA) in PBS at 4°C for 2 h. Lungs were embedded in paraffin and sectioned at 6 μm or embedded in OCT and sectioned at 10 μm. Histological analysis was performed as reported (Song et al., 2012).

Histology and immunohistochemistry was performed following standard procedures. The following primary antibodies were used: rabbit anti-NKX2.1 (Epitomics, 1:100), mouse anti-p63 (Santa Cruz, 1:100), goat anti-Clara cell 10-kDa protein (CC10) (Santa Cruz, 1:200), mouse anti-acetylated (Ac)-tubulin (Sigma, 1:1,000), rabbit anti-prosurfactant protein C (proSPC) (Millipore, 1:400), rabbit anti-mouse surfactant protein B (SPB) (Millipore, 1:200), mouse anti-DC-LAMP (Beckman, 1:200), hamster anti-T1α (Developmental Studies Hybridoma Bank, 1:200), rabbit anti-aquaporin 5 (AQP5) (Abcam,

1:200), mouse anti-Ki67 (BD Biosciences, 1:100), rabbit anti-phospho-Histone H3 (PH3) (Millipore, 1:200), rat anti-E-Cadherin (Life Technologies, 1:500). Secondary antibodies and conjugates used were donkey anti-rabbit Alexa Fluor 488 or 594 (Life Technologies, 1:1,000), donkey anti-goat Alexa Fluor 488, 594, or 647 (Life Technologies, 1:1,000), donkey anti-mouse Alexa Fluor 594 (Life Technologies, 1:1,000), and DAPI (Sigma, 1:10,000).

For biotinylated secondary antibodies (Jackson ImmunoResearch Laboratories, goat anti-hamster, 1:1000; goat anti-rabbit, 1:1,000; donkey anti-goat, 1:1,000; donkey anti-rat, 1:1000; and horse anti-mouse, 1:1,000), the signal was detected using streptavidin-conjugated Alexa Fluor 488, 594, or 647 (Life Technologies, 1:1000) or HRP-conjugated streptavidin (Perkin-Elmer, 1:1,000) in combination with either the chromogenic substrate DAB (Vector Laboratories) or fluorogenic substrate Alexa Fluor 488 tyramide (Perkin-Elmer, 1:200, TSA kit).

For PAS staining, paraffin sections were deparaffinized, oxidized in 0.5% periodic acid solution for 5 min and washed with distilled water. The sections were subsequently placed in Schiff reagent for 15 min, washed in tap water for 5 min and counterstained with Mayer's hematoxylin.

For BrdU or EdU incorporation, mice were injected with 1-2 mg of BrdU or EdU solution and lungs were collected 2-3 h following BrdU or EdU injection. BrdU staining was performed using the BrdU Staining Kit (Life Technologies). EdU staining was performed using the Click-iT® EdU Alexa Fluor 488 Imaging Kit (Life Technologies).

For TUNEL analysis, paraffin sections were deparaffinized and antigen retrieved. The sections were permeablized in PBS/0.5% Triton-X100 for 15 min, blocked in 3% BSA for 1 h at room temperature and incubated with rabbit anti-NKX2.1 antibodies (Epitomics) at 4°C overnight. Anti-rabbit Alexa Fluor 594 secondary antibodies (Molecular Probes) were added to the TUNEL reaction mix, which was prepared by diluting 1 part of Enzyme Solution in 9 parts of Label Solution from the *In Situ* Cell Death Detection Kit (Roche). The sections were incubated with the secondary antibody/TUNEL reaction mix for 1 h at 37°C, washed in PBS for three times, incubated with DAPI for 5 min and mounted in Vectashield for microscopy.

Fluorescent images were acquired using a SPOT 2.3 CCD camera connected to a Nikon E1000 epifluorescence microscope. Confocal images were captured on a Leica laser-scanning confocal microscope. Adjustment of red/green/blue histograms and channel merges were performed using SPOT Advanced software or ImageJ.

qPCR analysis

Total RNA was extracted from lung tissues using Trizol (Invitrogen) and subsequently reverse-transcribed using the Maxima First Strand cDNA Synthesis Kit (Thermo Scientific). Quantitative PCR (qPCR) was carried out on the ABI Prism 7900HT Sequence Detection System.

The following primers for mouse genes were used: *Gapdh* F: AGGTTGTCTCCTGCGACTTCA, *Gapdh* R: CCAG GAAATGAGCTTGACAAAGTT; *Ctgf* F: CTCCACCCGAGTTACCAATG, *Ctgf* R: TGGCGATTTTAGGTGTCCG; *Ajuba* F: GGTATCTATGGGCAGAGCAATG, *Ajuba* R: CAGTAGACAGAGCCATTGACG; *Cyr61* F: GTGAAGTGCGTCCTTGTGGACA, *Cyr61* R: CTTGACACTGGAGCATCCTGCA; *Foxa2* F: CGGGACTTAACTGTAACGGG, *Foxa2* R: TCATGTTGCTCACGGAAGAG; *Sftpc* (*SPC*) F: TCATGAAGATGGCTCCAGAGAGCA, *Sftpc* R: ACTCGGAACCAGTATCATGCCCTT; *Sftpb* (*SPB*) F: AGAATGGCCACTACAGGACACTGA, *Sftpb* R: GGCATGTGCTGTTCCACAAACTGT, *Abca3* F: CTTCATGGACGAAGCTGACCTG, *Abca3* R: GTGCGGTTCTTTTACCAGCGTC, *Pdpn* F: TGAATCTACTGGCAAGGCACCTCT, *Pdpn* R: GGTGACTACTGGCAAGCCATCTTT; *Aqp5* F: AGCAACAACACAACACCAGGCAAG, *Aqp5* R: TCATGGAACAGCCGGTGAAGTAGA; *Scgb1a1* (*CC10)* F: AGTCTGGTTATGTGGCATCCCTGA, *Scgb1a1* R: ACACAGGGCAGTGACAAGGCTTTA; *Foxj1* F: AAGGTAACTTTGACTGGGAGGCCA, *Foxj1* R: AGGATGTGGCCAAGAAGGTCTCAT; *Calca* (*CGRP*) F: TGTCAGCATCTTGCTCCTGTACCA, *Calca* R: TGGCAGTGTTGCAGGATCTCTTCT; *Trp63* (*p63*) F: TGGCATTAGCCATAGGTAGGCACA, *Trp63* R: TCACCACCAAGTGAAGGAATCCCA.

The following primers for human genes were used: *GAPDH* F: AAGGTGAAGGTCGGAGTC, *GAPDH* R: GATTTTGGAGGGATCTCG; *SFTPC* F: AGCCAGAAACACACGGAGATGGTT, *SFTPC* R: ATCTTCATGATGTAGCAGCAGGTGCC; *SFTPB* F: TCCTTAACAAGATGGCCAAGGAGG, *SFTPB* R: TGCCGTTTGAGTCAGTCTGGTTCT;

Western blot analysis

Embryonic lung tissues were homogenized in RIPA buffer supplemented with Complete Protease Inhibitor Cocktail tablets (Roche) and phosSTOP Phosphatase Inhibitor Cocktail tablets (Roche). The lysates were cleared and analyzed by Western blot as previously described (Lin et al., 2012).

The following primary antibodies were used: rabbit anti-YAP (Cell Signaling, 1:500), rabbit anti-phospho-YAP (Cell Signaling, 1:1000), rabbit anti-LATS (Cell Signaling, 1:1000), rabbit anti-phospho-LATS (Cell Signaling, 1:1000), rabbit anti-MST1 (Cell Signaling, 1:500), rabbit anti-MST2 (Cell Signaling, 1:1000), goat anti-MST1/2 (Santa Cruz 1:100), goat anti-CTGF (Santa Cruz, 1:200).

Genome-wide identification of conserved TEAD-binding sites in gene promoters

Searching for putative TEAD-binding sites (GGAATG) on mouse gene promoters (−500 to 0; transcription start as +1) was performed using the Regulatory Sequence Analysis Tools (RSAT) (http://rsat.ulb.ac.be/rsat/) and implemented with the pattern matching tool. The

conservation of the cis-regulatory elements identified was assessed using the "Conservation" track from the UCSC browser (http://genome.ucsc.edu/).

shRNA-mediated knockdown in cell lines

shRNAs were designed using pSicOligomaker (Reynolds et al., 2004) and oligonucleotides encoding shRNAs were cloned into the pLentiLox3.7 vector. Lentiviruses were produced as described (Chen et al., 2009). A549 and MLE 12 cells at 50% confluence were transduced with lentiviruses supplemented with 8μg/ml polybrene. Upon reaching confluence, the cells were collected for RNA and protein extraction. The following 19-mer target sequences were used for shRNA-mediated knockdown: GTACAAGGCTATTCATAAA and GCAGGTCAACTTACAGATA for mouse *Mst1* (NM_021420); GTCAAGTGGTTGCAATTAA and GTACACACCTAGATAAATT for mouse *Mst2* (NM_019635); GGAGAAGTTTACTACATAA and GTAGTGTGATAGCAGAATA for mouse *Yap* (NM_009534); GCCAGATTGTTGCTATTAA for human *MST1* (NM_006282); GTCAAGTTGTCGCAATTAA for human *MST2* (NM_006281); GAAGTAGTTTAGTGTTCTA for human *YAP* (NM_006106).

Results

Inactivation of Mst1/2 by Nkx2.1-Cre in mice leads to postnatal lethality and lung defects

We took advantage of a null allele of *Mst1* (denoted $Mst1^{-}$) and a conditional (floxed) allele of *Mst2* ($Mst2^{f}$) (Song et al., 2010) to study the function of *Mst1/2* in the lung. As a first step, we utilized *Nkx2.1-Cre* (Xu et al., 2008) to inactivate *Mst2* in the lung epithelium since *Nkx2.1* is expressed in all lung endodermal cells. We found that $Mst1^{-/-}; Mst2^{f/f}; Nkx2.1^{Cre/+}$ mice (carrying one transgenic allele of *Nkx2.1-Cre*) were viable and fertile without apparent gross abnormalities (Fig. 1A, B, E, F). By contrast, $Mst1^{-/-}; Mst2^{f/f}; Nkx2.1^{Cre/Cre}$ mice (carrying two alleles of *Nkx2.1-Cre*) exhibited various phenotypes postnatally (Fig. 1A, C, E, G). At birth, they cannot be distinguished from their wild-type littermates by external morphology but subsequently became visibly smaller in size and appeared emaciated. These mice died at various time points after birth; most of them perished before they reached 3 weeks of age although a few survived beyond that (Fig, 1I, J, K). These findings are largely similar to reports on $Mst1^{f/f}; Mst2^{-/-}$ mice that also carry *Nkx2.1-Cre* (Chung et al., 2013). In that study, a conditional allele of *Mst1* ($Mst1^{f}$) (Katagiri et al., 2009) and a null allele of *Mst2* ($Mst2^{-}$) (Oh et al., 2009) were utilized to assess the functional consequence of *Mst1/2* removal in the lung.

As expected from their reduced postnatal survival, $Mst1^{-/-}; Mst2^{f/f}; Nkx2.1^{Cre/Cre}$ mice displayed more severe lung defects than those in $Mst1^{-/-}; Mst2^{f/f}; Nkx2.1^{Cre/+}$ mice in our study (Fig. 1B, C, F, G). Upon gross examination, we noticed regions of lungs at the upper lobes that lost the normal color and architecture in both $Mst1^{-/-}; Mst2^{f/f}; Nkx2.1^{Cre/+}$ and $Mst1^{-/-}; Mst2^{f/f}; Nkx2.1^{Cre/Cre}$ mice (Fig. 1B, C; Fig. S1). These affected regions were more extensive in $Mst1^{-/-}; Mst2^{f/f}; Nkx2.1^{Cre/Cre}$ lungs. Microscopically, a significantly larger number of extra lung cells were present in $Mst1^{-/-}; Mst2^{f/f}; Nkx2.1^{Cre/Cre}$ lungs than in $Mst1^{-/-}; Mst2^{f/f}; Nkx2.1^{Cre/+}$ lungs (Fig. 1F, G).

Elimination of Mst1/2 by Shh-Cre in mice results in neonatal lethality and more severe lung phenotypes

In other studies that utilize epithelial mouse Cre lines to inactivate conditional alleles, we noticed that *Nkx2.1-Cre* (Xu et al., 2008) was less efficient than *Shh-Cre* (Harfe et al., 2004) in converting a conditional allele into a null allele. We wondered whether the lung defects in *Mst1*$^{-/-}$*; Mst2*$^{f/f}$*; Nkx2.1*$^{Cre/Cre}$ mice represented a partial loss of *Mst1/2* function in the lung epithelium and lung defects associated with complete elimination of *Mst1/2* function has not been revealed. To address this issue, we employed *Shh-Cre*, which seems to exhibit a high efficiency in the lung epithelium, to remove *Mst1/2* in the lung.

Taking a similar approach, we generated *Mst1*$^{-/-}$*; Mst2*$^{f/f}$*; Shh*$^{Cre/+}$ mice (carrying one knock-in allele of *Shh-Cre*). Of note, *Mst1*$^{-/-}$*; Mst2*$^{f/f}$*; Shh*$^{Cre/Cre}$ mice (carrying two alleles of *Shh-Cre*) exhibited the classical Hedgehog phenotypes, including cyclopia, holoprosencephaly and limb and lung defects, due to disruption of the *Shh* locus and these animals died at various time points during embryonic development as previously reported (Chiang et al., 1996). *Mst1*$^{-/-}$*; Mst2*$^{f/f}$*; Shh*$^{Cre/+}$ mice died soon after birth although they could not be distinguished from their wild-type littermates by external morphology. The dying pups were gasping for air, suggesting that they suffered from respiratory distress. Inspection of their lungs revealed only small pockets of air, indicating a failure of lung expansion after birth that resulted in neonatal lethality (Fig. 1A, D). On rare occasions, some *Mst1*$^{-/-}$*; Mst2*$^{f/f}$*; Shh*$^{Cre/+}$ mice (~5%) escaped neonatal lethality. These escapers could die within three weeks of age but most of them reached adulthood although some of these adult escapers still displayed varying degrees of lung defects (Fig. 1I, L). In contrast to the postnatal lethality in *Mst1*$^{-/-}$*; Mst2*$^{f/f}$*; Nkx2.1*$^{Cre/Cre}$ mice, the neonatal lethality observed in most *Mst1*$^{-/-}$*; Mst2*$^{f/f}$*; Shh*$^{Cre/+}$ mice suggest a more severe lung defect in these animals (Fig. 1E, F, G, H). This confirms our speculation that efficient removal of *Mst1/2* using *Shh-Cre* is required to uncover the phenotypes associated with a more complete loss of *Mst1/2* function in the lung epithelium. Consistent with this, analysis of MST2 protein from *Mst1*$^{-/-}$*; Mst2*$^{f/f}$*; Shh*$^{Cre/+}$ lungs at 16.5 and 18.5 *days post coitus* (*dpc*) revealed significantly reduced MST2 protein levels (Fig. S2). The residual MST2 protein likely comes from the lung mesenchyme since *Shh-Cre* is not expressed in the mesenchymal compartment. Importantly, MST2 protein levels were reduced to a lower level in *Mst1*$^{-/-}$*; Mst2*$^{f/f}$*; Shh*$^{Cre/+}$ lungs than *Mst1*$^{-/-}$*; Mst2*$^{f/f}$*; Nkx2.1*$^{Cre/Cre}$ lungs (Fig. S2), supporting the notion that Shh-Cre is more efficient than Nkx2.1-Cre in converting *Mst2*^{f} to a null allele.

Analysis of Mst1$^{-/-}$; Mst2$^{f/f}$; Shh$^{Cre/+}$ and Mst1$^{-/-}$; Mst2$^{f/f}$; Nkx2.1$^{Cre/Cre}$ lungs reveals increased cell proliferation and disrupted lung cell differentiation

We performed a detailed phenotypic analysis of lungs from *Mst1*$^{-/-}$*; Mst2*$^{f/f}$*; Shh*$^{Cre/+}$ mice. We found that *Mst1*$^{-/-}$*; Mst2*$^{f/f}$*; Shh*$^{Cre/+}$ lungs at 18.5 *dpc* or postnatal day 0 (P0) had reduced airway space (Fig. 1D, H; Fig. S3). In addition, the mutant lungs had a more compact appearance likely due to the presence of more lung cells. Compared with *Mst1*$^{-/-}$*; Mst2*$^{f/f}$*; Nkx2.1*$^{Cre/+}$ or *Mst1*$^{-/-}$*; Mst2*$^{f/f}$*; Nkx2.1*$^{Cre/Cre}$ lungs, *Mst1*$^{-/-}$*; Mst2*$^{f/f}$*; Shh*$^{Cre/+}$ lungs appeared denser and possessed a larger number of lung cells (Fig. 1E, F, G, H).

We determined the rate of cell proliferation in *Mst1*$^{-/-}$*; Mst2*$^{f/f}$*; Shh*$^{Cre/+}$ lungs by BrdU or EdU incorporation. Epithelial cells were distinguished by staining with E-cadherin antibody (Fig, 2Y, Z). We found that the number of BrdU^{+} or EdU^{+} cells was increased in the epithelium of *Mst1*$^{-/-}$*; Mst2*$^{f/f}$*; Shh*$^{Cre/+}$ lungs at 18.5 *dpc* (Fig. 2A'). Interestingly, expression of cell cycle regulators, such as *Mycn* (N-myc) and *Ccnd2* (cyclin D2) was elevated in *Mst1*$^{-/-}$*; Mst2*$^{f/f}$*; Shh*$^{Cre/+}$ lungs (Fig. 3A). These results suggest that increased cell proliferation in the absence of *Mst1/2* could account for the increased cell number and denser lung morphology. In support of this notion, in many bronchioles, the simple columnar epithelium in wild-type lungs (Fig. 2I) was replaced by pseudostratified epithelium in *Mst1*$^{-/-}$*; Mst2*$^{f/f}$*; Shh*$^{Cre/+}$ lungs (Fig. 2L). Expression of cell cycle regulators was also increased in *Mst1*$^{-/-}$*; Mst2*$^{f/f}$*; Nkx2.1*$^{Cre/Cre}$ lungs (Fig. 3B), consistent with the presence of extra lung cells. By contrast, the rate of cell death was not significantly altered in the absence of *Mst1/2* (Fig. S4).

The lung epithelial cells were marked by NKX2.1 in *Mst1*$^{-/-}$*; Mst2*$^{f/f}$*; Shh*$^{Cre/+}$ lungs in a pattern similar to that of control lungs at 18.5 *dpc*, suggesting that the lung epithelial cell fate is unaffected in the absence of *Mst1/2* (Fig. S4). Analysis of marker expression in *Mst1*$^{-/-}$*; Mst2*$^{f/f}$*; Shh*$^{Cre/+}$ lungs at 18.5 *dpc* and P0 revealed partial disruption of differentiation in lung epithelium. Major lung cell types including Clara [club] cells (CC10^{+}), ciliated cells (Acetylated [Ac]-tubulin^{+}), goblet cells (PAS^{+}), basal cells (p63^{+}), alveolar type II (SPC^{+}, DC-LAMP^{+}) and type I cells (T1α^{+}, AQP5^{+}) cells were present (Fig. 2A-P; Fig. S3); however, Clara cells and ciliated cells were relatively sparse (Fig. 2D, J, Q; Fig. S3). This is consistent with reduced levels of *CC10* (Clara cell) and *Foxj1* (ciliated cell) mRNA in *Mst1*$^{-/-}$*; Mst2f/f; Shh*$^{Cre/+}$ lungs (Fig. 3C). The number of alveolar type II cells was also decreased in *Mst1*$^{-/-}$*; Mst2*$^{f/f}$*; Shh*$^{Cre/+}$ lungs (Fig. 2E, K, Q). Interestingly, we noticed reduced *SPB/SPC/Abca3* (type II cell) mRNA expression while *Pdpn* (*T1α*)/*Aqp5* (type I cell) mRNA levels were elevated (Fig. 3C), suggesting defects in alveolar cell development or maturation. Dense lung architecture and reduced surfactant production likely prevented normal lung expansion and caused neonatal lethality.

Similar results were obtained in *Mst1*$^{-/-}$*; Mst2*$^{f/f}$*; Nkx2.1*$^{Cre/Cre}$ lungs in which the number of Clara cells and ciliated cells was significantly reduced (Fig. 2R, W; Fig. S3); alveolar type I and type II cells could be readily detected (Fig, 2S, X; Fig. S3). Moreover, expression of *CC10*, *Foxj1*, *SPB*, *SPC* and *Abca3* was reduced while the transcript levels of *Pdpn* and *Aqp5* were elevated in *Mst1*$^{-/-}$*; Mst2*$^{f/f}$*; Nkx2.1*$^{Cre/Cre}$ lungs (Fig. 3D). By contrast, changes in lung epithelial cell number were not apparent in *Mst1*$^{-/-}$*; Mst2*$^{f/f}$*; Nkx2.1*$^{Cre/+}$ lungs (Fig. 2T-V), correlated with their mild lung phenotypes and lack of postnatal lethality.

These results indicate that while loss of *Mst1/2* did not interfere with lobation or branching, the correct number of lung epithelial cells failed to be produced. This likely reflects partial disruption of coordinated lung epithelial cell proliferation and differentiation in the absence of MST1/2 activity.

Hippo target genes are upregulated in $Mst1^{-/-}$; $Mst2^{f/f}$; $Shh^{Cre/+}$ and $Mst1^{-/-}$; $Mst2^{f/f}$; $Nkx2.1^{Cre/Cre}$ lungs

To characterize the molecular defects in *Mst1/2* mutant lungs, we asked whether expression of YAP targets was affected in the absence of *Mst1/2*. We extracted RNA from *Mst1*$^{-/-}$; *Mst2*$^{f/f}$; *Shh*$^{Cre/+}$ lungs at 16.5 and 18.5 *dpc* and examined the expression of Hippo targets by qPCR analysis and Western blotting. We found that mRNA levels of well-documented YAP targets, such as *Ctgf* (connective tissue growth factor, Ccn2) and *Cyr61* (cysteine rich protein 61, CCN1) (Chan et al., 2011; Zhang et al., 2009; Zhao et al., 2008), were significantly elevated in the mutant lungs (Fig. 3E). CTGF protein levels were also increased in *Mst1*$^{-/-}$; *Mst2*$^{f/f}$; *Shh*$^{Cre/+}$ lungs at 16.5 and 18.5 *dpc* (Fig. 3G; Fig. S5). These results provide strong evidence to support increased YAP activity in *Mst1/2*-deficient lungs.

To confirm increased YAP activity in the absence of *Mst1/2*, we searched for additional YAP target genes in the lung. We conducted a genome-wide promoter analysis using the Regulatory Sequence Analysis Tools (RSAT) to identify genes that contain conserved TEAD-binding sites in their promoters. Candidates were further tested in a mouse lung epithelial cell line, MLE 12 (Wikenheiser et al., 1993), for induced expression by YAP^{S5A}, an active form of YAP in which five LATS phosphorylation sites are removed (Zhao et al., 2007). We found that overexpression of YAP^{S5A} in mouse MLE 12 cells increased expression of *Ajuba* (ajuba LIM protein), *Lamc2* (laminin, gamma 2) and *Prkci* (protein kinase C, iota), suggesting that *Ajuba*, *Lamc2* and *Prkci* are direct YAP targets (Fig. S6). As expected, *Ajuba*, *Lamc2* and *Prkci* were also upregulated in *Mst1*$^{-/-}$; *Mst2*$^{f/f}$; *Shh*$^{Cre/+}$ lungs (Fig. 3E). Taken together, these observations suggest that YAP targets are upregulated as a consequence of *Mst1/2* deletion.

We also examined the expression levels of *Foxa2* in *Mst1*$^{-/-}$; *Mst2*$^{f/f}$; *Shh*$^{Cre/+}$ lungs by qPCR and found that *Foxa2* was slightly reduced (data not shown). Whether *Foxa2* mediates some aspects of *Mst1/2* function in the lung is unclear.

We also extracted RNA from *Mst1*$^{-/-}$; *Mst2*$^{f/f}$; *Nkx2.1*$^{Cre/Cre}$ lungs and performed similar assays. We focused analysis on postnatal *Mst1*$^{-/-}$; *Mst2*$^{f/f}$; *Nkx2.1*$^{Cre/Cre}$ lungs since the cumulative effects of Nkx2.1-Cre over time likely result in more complete *Mst2* removal and enable the detection of molecular perturbations. Hippo targets (*e.g.*, *Ctgf*, *Ajuba*, *Cyr61*, *Lamc2* and *Prkci*) were also upregulated in *Mst1*$^{-/-}$; *Mst2*$^{f/f}$; *Nkx2.1*$^{Cre/Cre}$ lungs (Fig. 3F) although upregulation of *Ctgf* was less pronounced than that in *Mst1*$^{-/-}$; *Mst2*$^{f/f}$; *Shh*$^{Cre/+}$ lungs (Fig. 3E). Likewise, CTGF protein levels were increased in *Mst1*$^{-/-}$; *Mst2*$^{f/f}$; *Nkx2.1*$^{Cre/Cre}$ lungs (Fig. 3H). These findings suggest that although the efficiency of *Mst1/2* inactivation may differ among mouse Cre lines, increased YAP target gene expression due to loss of *Mst1/2* in the lung epithelium is a common consequence.

A relative reduction in phospho-Yap protein levels is detected in $Mst1^{-/-}$; $Mst2^{f/f}$; $Shh^{Cre/+}$ and $Mst1^{-/-}$; $Mst2^{f/f}$; $Nkx2.1^{Cre/Cre}$ lungs

If a conserved MST1/2-YAP cascade is utilized during lung growth, we anticipate a reduction in phospho-YAP protein levels (relative to total YAP) in *Mst1/2*-deficient lungs since phosphorylation of YAP protein would be diminished due to inactivation of *Mst1/2*.

To test these predictions, we isolated proteins from *Mst1*$^{-/-}$; *Mst2*$^{f/f}$; *Shh*$^{Cre/+}$ lungs at 16.5 and 18.5 *dpc* and studied the protein levels of total YAP and phospho-YAP (S127) by Western blotting. Indeed, loss of *Mst1/2* was accompanied by a relative decrease in phospho-YAP protein levels (normalized to total YAP) (Fig. 3G; Fig. S5). This is consistent with a model in which elimination of *Mst1/2* relieves YAP protein phosphorylation and degradation in the cytoplasm. Increased protein levels of active (non-phosphorylated) YAP in the absence of Mst1/2 could lead to upregulation of YAP target gene expression. We noticed that in some *Mst1*$^{-/-}$; *Mst2*$^{f/f}$; *Shh*$^{Cre/+}$ animals, the correlation between loss of *Mst1/2* and the total YAP and phospho-YAP protein levels was not evident. Perhaps, these animals had milder perturbation of Hippo signaling and some of them may even escape neonatal lethality. This was further complicated by assays using the whole lung, which could obscure minor changes in epithelial Yap protein levels caused by loss of *Mst1/2*.

Since Yap targets were also elevated in *Mst1*$^{-/-}$; *Mst2*$^{f/f}$; *Nkx2.1*$^{Cre/Cre}$ lungs, we expected changes in YAP protein that reflect its increased activity. To explore this idea, we isolated proteins from *Mst1*$^{-/-}$; *Mst2*$^{f/f}$; *Nkx2.1*$^{Cre/Cre}$ lungs and determined the expression of total YAP and phospho-YAP (S127) by Western blotting. We found variable expression levels of total YAP and phospho-YAP (S127) in different animals. Nevertheless, loss of *Mst1/2* was also accompanied by a relative decrease in phospho-YAP protein levels (normalized to total YAP) in the lung (Fig. 3H). This is similar to findings in *Mst1*$^{-/-}$; *Mst2*$^{f/f}$; *Shh*$^{Cre/+}$ lungs. In some *Mst1*$^{-/-}$; *Mst2*$^{f/f}$; *Nkx2.1*$^{Cre/Cre}$ animals, the correlation between loss of *Mst1/2* and the total YAP and phospho-YAP protein levels was not apparent. We surmise that the weaker and variable activity of Nkx2.1-Cre in the lung in conjunction with the use of the whole lung for analysis could have contributed to fluctuating YAP protein levels in *Mst1*$^{-/-}$; *Mst2*$^{f/f}$; *Nkx2.1*$^{Cre/Cre}$ lungs.

In the canonical Hippo pathway, LATS has been proposed to mediate the function of MST1/2 in controlling YAP activity. In this model, the MST1/2 kinases phosphorylate the LATS kinase, which in turn phosphorylates YAP. This linear pathway seems to be highly context-dependent and variations have been found in some tissues or cell lines studied (Zhou et al., 2009). To test whether LATS relays MST1/2 activity in the lung, we examined the protein levels of total LATS and phospho-LATS in *Mst1/2*-deficient lungs by Western blotting. Both total LATS and phospho-LATS protein levels were largely unaltered in *Mst1*$^{-/-}$; *Mst2*$^{f/f}$; *Shh*$^{Cre/+}$ lungs at either 16.5 or 18.5 *dpc* or *Mst1*$^{-/-}$; *Mst2*$^{f/f}$; *Nkx2.1*$^{Cre/Cre}$ lungs at P2 (Fig. 3G, H and data not shown). We speculate that minor changes in epithelial LATS protein phosphorylation caused by loss of *Mst1/2* were masked since LATS from the whole lung was analyzed. However, we cannot exclude the possibility that LATS controls YAP activity but LATS activation is not correlated with changes in its protein levels or phosphorylation states in the lung. Finally, MST1/2 may exploit a player other than LATS to modify YAP activity during lung growth.

Removal of one allele of Yap or one copy of both Yap and Taz can rescue neonatal lethality and lung defects induced by loss of Mst1/2 by Shh-Cre in the lung epithelium

To provide a more definitive answer to the regulatory relationship between MST1/2 and YAP in the lung, we performed genetic rescue experiments. We reasoned that if the neonatal

lethality and lung phenotypes observed in *Mst1*$^{-/-}$*; Mst2*$^{f/f}$*; Shh*$^{Cre/+}$ mice are due to increased YAP and/or TAZ function, reduction of *Yap/Taz* gene dosage should normalize YAP/TAZ activity and restore proper Hippo signaling. To this end, we employed conditional alleles of *Yap* (*Yap*^{f}) (Xin et al., 2011) and *Taz* (*Taz*^{f}) (Xin et al., 2013) and set up crosses to obtain *Mst1*$^{-/-}$*; Mst2*$^{f/f}$*; Yap*$^{f/+}$*; Taz*$^{f/+}$*; Shh*$^{Cre/+}$ mice. Shh-Cre would convert *Yap*^{f} and *Taz*^{f} into null alleles and reduce YAP/TAZ activity. Indeed, no neonatal lethality was observed in *Mst1*$^{-/-}$*; Mst2*$^{f/f}$*; Yap*$^{f/+}$*; Taz*$^{f/+}$*; Shh*$^{Cre/+}$ mice and they survived to adulthood without obvious lung phenotypes compared to their wild-type littermates (Fig. 4A-P). No apparent defects in lung epithelial cell specification were detected in these animals (Fig. 4A-P). This suggests that the activity of the nuclear effectors of MST1/2 (i.e. YAP/TAZ) is reduced to the extent that expression of Hippo target genes are no longer upregulated to disrupt lung development.

We also tested whether removing one copy of *Yap* is sufficient to rescue the neonatal lethality in the absence of *Mst1/2*. Somewhat surprisingly, similar to *Yap*$^{f/+}$*; Taz*$^{f/+}$*; Shh*$^{Cre/+}$ mice, *Mst1*$^{-/-}$*; Mst2*$^{f/f}$*; Yap*$^{f/+}$*; Shh*$^{Cre/+}$ mice also survived to adulthood without discernable lung phenotypes compared to their wild-type littermates (Fig. 5A-P). This is consistent with the model in which YAP plays a more dominant role than TAZ in the Hippo pathway during lung development. Thus, in the absence of *Mst1/2*, removal of one copy of *Yap* reduces YAP activity to the level that enables proper Hippo signaling and lung development. Taken together, our findings provide strong genetic evidence to support a conserved MST1/2-YAP/TAZ axis in controlling lung development.

Knockdown of Mst1/2 in alveolar lung cell lines leads to elevated Yap target and reduced alveolar marker expression, which can be restored by inactivating Yap

To complement the genetic studies, we employed cell-based assays and used A549 (Lieber et al., 1976) and MLE 12 cells (Wikenheiser et al., 1993) to further probe the relationship between MST1/2 and YAP. The human A549 lung cell line is widely used as an *in vitro* model for alveolar type II cells while the mouse MLE 12 lung cell line maintains properties of distal respiratory epithelial cells and expresses surfactant proteins. A549 and MLE 12 cells were transduced with lentiviruses that carry shRNA against *Mst1/2* (Fig. 6A, B). Knockdown of *Mst1/2* was assessed by Western blotting. We found that reduced *Mst1/2* expression in cultured cells led to increased expression of YAP targets such as CTGF (Fig. 6B). Interestingly, expression of alveolar markers such as *SPB/SPC* was reduced when *Mst1/2* were inactivated in lung cells (Fig. 6A), similar to findings obtained in *Mst1/2* deficient lungs (Fig. 3C, D). Importantly, elevated YAP target and reduced *SPB/SPC* expression was abolished when *Yap* was simultaneously knocked down in conjunction with *Mst1/2* (Fig. 6A, B). These results are consistent with negative regulation of YAP targets by MST1/2 in lung cell lines and further support a conserved MST1/2-YAP axis during lung growth (Fig. 7).

Discussion

Our studies clarify the regulatory relationship between MST1/2 and YAP during lung growth and development. Through a combination of phenotypic analysis, genetic epistasis,

molecular characterization and cell-based assays, we define a conserved MST1/2-YAP axis in regulating lung growth. These results also establish the foundation for future investigations to uncover the genetic and molecular interactions of Hippo pathway components during lung development and homeostasis and in lung diseases.

Control of YAP activity by MST1/2 appears to be context-dependent (Varelas, 2014). In the liver, pancreas, heart and nervous system, a classical MST1/2-YAP axis mediates critical aspects of Hippo signaling. Our work shows that a similar MST1/2-YAP axis also operates during lung growth. By contrast, MST1/2 are found to function independently of YAP in the skin (Schlegelmilch et al., 2011) and kidney (Reginensi et al., 2013) and in mouse embryonic fibroblasts (MEFs) (Zhou et al., 2009). This is in contrast to other major signaling pathways, which utilize a common signaling cascade in diverse tissues and cell lines. This unique aspect of Hippo signaling could reflect the distinct signal input and integration that Hippo signaling needs to accommodate in a given tissue. As a result, MST1/2 and YAP may be subject to differential regulation in some tissues and no longer exhibit a direct regulatory relationship.

Our analysis of *Mst1/2*-deficient lungs demonstrates upregulation of YAP targets, including the well-established targets, *Ctgf* and *Cyr61*, and new YAP targets, *Ajuba*, *Lamc2* and *Prkci*, in the absence of *Mst1/2*. This is associated with a relative reduction in phospho-YAP protein levels. Together, these findings provide strong evidence to support negative regulation of YAP by MST1/2. Consistent with the expected difference in Cre activity, MST2 protein reduction is more complete and upregulation of YAP targets more pronounced in lungs in which *Mst1/2* are removed by *Shh-Cre* than those induced by *Nkx2.1-Cre* in our investigation. Of note, a recent study (Chung et al., 2013) reported reduced YAP, CTGF and FOXA2 protein levels in lungs derived from $Mst1^{f/f}; Mst2^{-/-}$ mice that carry *Nkx2.1-Cre*. It is unclear how this discrepancy has arisen. Perhaps the mouse genetic background, the use of different *Mst1/2* alleles and the allelic combination of *Mst1* conditional/*Mst2* null versus *Mst2* conditional/*Mst1* null alleles could have influenced YAP target gene expression in different studies. We found that *Foxa2* expression levels were slightly reduced in $Mst1^{-/-}; Mst2^{f/f}; Shh^{Cre/+}$ lungs by qPCR. Whether *Foxa2* mediates some aspects of *Mst1/2* function in the lung requires additional studies. It is interesting to note that removal of *Foxa2* in lung epithelium affects alveolarization but not branching morphogenesis (Wan et al., 2004) while epithelial deletion of both *Foxa1* and *Foxa2* inhibits branching morphogenesis (Wan et al., 2005).

While a relative reduction in phospho-YAP protein levels was observed in *Mst1/2*-deficient lungs, variations in YAP and phospho-YAP protein levels were noted in different litters of mice. This could be caused by variable Cre activity but it could also be due to additional YAP regulators other than MST1/2 in the lung. Moreover, YAP from both lung epithelium and mesenchyme was detected in our assays and this may have masked small changes in YAP protein levels in the epithelium. While isolated lung epithelial cells would provide a more accurate assessment of changes in YAP protein levels, it is unclear how manipulation of the lung epithelium such as disruption of cell junctions for cell isolation and sorting would affect YAP protein expression. In contrast to altered YAP protein levels in *Mst1/2*-deficient lungs, protein levels of phospho-LATS seem to be unaltered. It is very likely that a

minor shift in epithelial LATS protein levels was obscured in assays using the whole lung as described above. Nevertheless, we cannot rule out the possibility that LATS may control YAP activity but LATS activation is not correlated with changes in its protein levels or phosphorylation states in the lung. Moreover, MST1/2 may employ kinases other than LATS to modify YAP in the lung. The lack of a linear relationship between MST1/2, LATS and YAP has been reported in other tissues (such as the liver) (Zhou et al., 2009). These findings highlight the context-dependent interactions between Hippo pathway components. They also underscore the importance of studying Hippo signaling in tissues and organs to uncover its function in a physiological setting.

Our analysis of *Mst1*$^{-/-}$*; Mst2*$^{f/f}$*; Yap*$^{f/+}$*; Shh*$^{Cre/+}$ and *Mst1*$^{-/-}$*; Mst2*$^{f/f}$*; Yap*$^{f/+}$*; Taz*$^{f/+}$*; Shh*$^{Cre/+}$ mice provides strong genetic evidence to support a conserved MST1/2-YAP/TAZ axis in regulating lung development. We predict that mice expressing active forms of YAP (such as YAP^{S127A} or YAP^{S5A}) would display phenotypes similar to those in *Mst1/2*-deficient lungs. Furthermore, genetic analysis of the lung phenotypes in *Lats* mutant mice in conjunction with double mutant analysis would shed light on the relationship between *Mst1/2*, *Lats* and *Yap* in the lung. These genetic studies will complement cell-based assays in delineating the interactions of Hippo pathway components in the respiratory system.

Nkx2.1-Cre is presumably expressed from the earliest time point of lung development and *Nkx2.1-Cre* can label most, if not all, lung epithelial cells (Song et al., 2012). It is thus somewhat surprising that *Nkx2.1-Cre* is less efficient in removing *Mst1/2* in lung epithelium than *Shh-Cre*. We speculate that this could be due to the expression levels of *Nkx2.1-Cre*. Indeed, mice carrying two alleles of *Nkx2.1-Cre* display more severe lung phenotypes caused by *Mst1/2* deletion than those with only one *Nkx2.1-Cre* allele. Moreover, *Nkx2.1-Cre* may be expressed at higher levels at the upper lung lobes or these regions are more sensitive to loss of *Mst1/2* activity since the lung phenotypes are more severe in these areas. Even if the cumulative effects of Nkx2.1-Cre activity eventually result in apparent removal of *Mst1/2* at birth, residual *Mst1/2* function during lung development could be sufficient to support substantial lung growth. Finally, we anticipate that *Nkx2.1-Cre* would be less efficient in general than *Shh-Cre* in converting a conditional allele to a null allele in the lung epithelium. It is unclear whether this is due to mosaic expression from transgenic mouse lines or it reflects the expression levels of individual promoter activity. A combined use of different epithelial Cre lines thus offers a unique opportunity to reveal a spectrum of phenotypes and uncover the molecular basis of these defects.

Both *Nkx2.1-Cre* and *Shh-Cre* display extrapulmonary expression. The brains of *Mst1*$^{-/-}$*; Mst2*$^{f/f}$*; Nkx2.1*$^{Cre/Cre}$ or *Mst1*$^{-/-}$*; Mst2*$^{f/f}$*; Shh*$^{Cre/+}$ mice do not exhibit gross morphological defects. While we cannot rule out specific brain defects in these mice, we surmise that postnatal lethality in *Mst1*$^{-/-}$*; Mst2*$^{f/f}$*; Nkx2.1*$^{Cre/Cre}$ mice and neonatal lethality in *Mst1*$^{-/-}$*; Mst2*$^{f/f}$*; Shh*$^{Cre/+}$ mice are due to lung defects and not caused by dysfunction of the nervous system. It is somewhat unexpected that a small number of *Mst1*$^{-/-}$*; Mst2*$^{f/f}$*; Shh*$^{Cre/+}$ mice survive postnatally since phenotypes associated with the conversion of other conditional alleles to null alleles using *Shh-Cre* appear to be highly penetrant. This may reflect variable Shh-Cre-mediated excision in different animals and/or the influence of genetic background. It could also suggest the ability of the animals to tolerate a high degree of YAP activation

before phenotypic consequences are revealed. Further analysis of surviving *Mst1*$^{-/-}$; *Mst2*$^{f/f}$; *Nkx2.1*$^{Cre/Cre}$ or *Mst1*$^{-/-}$; *Mst2*$^{f/f}$; *Shh*$^{Cre/+}$ mice could yield new insight into how Hippo signaling controls lung development and maturation.

Loss of *Mst1/2* leads to increased YAP target gene expression. How the activation of YAP targets controls diverse aspects of lung cell behavior has not been elucidated. Conversely, the molecular mechanisms by which loss of YAP affects lung branching morphogenesis remain unclear. YAP targets likely mediate central aspects of YAP activity. In this regard, the newly identified YAP targets, *Lamc2* and *Prkci*, are potential candidates to link Hippo signaling to cellular microenvironment. It is uncertain how increased Hippo signaling activity disrupts the normal process of lung cell proliferation/differentiation and compromises the production of a proper number of distinct lung cell types. Perhaps, accelerated cell proliferation and perturbed cell differentiation caused by loss of *Mst1/2* collectively result in an imbalance of cell type production. Thus, the number of some lung cell types is significantly reduced. To gain further insight into these important issues requires future studies to trace the lineage and fates of *Mst1/2*-deficient epithelial cells during lung development and to identify genes and pathways perturbed due to the disruption of *Mst1/2*. Since MST1/2 likely control a plethora of targets, it is likely that multiple YAP targets rather than one target would mediate the effects of MST1/2. Moreover, MST1/2 and YAP may function in a complex network in tissues; *Mst1/2* regulate genes other than *Yap* and conversely YAP receives signals other than MST1/2. Uncovering the functions of genes and pathways regulated by MST1/2 and YAP during lung development will increase our mechanistic understanding of how Hippo signaling controls lung growth.

Many genes and pathways that control lung development have been identified (Borok et al., 2011; Dobbs et al., 2010; Domyan and Sun, 2011; Hardie et al., 2010; Herriges and Morrisey, 2014; Kotton, 2012; Morrisey et al., 2013; Ornitz and Yin, 2012; Shi et al., 2009; Warburton et al., 2010). Whether and how these major pathways participate in lung growth control requires additional studies. Since lung growth is a tightly controlled process, we speculate that a master regulatory pathway is required to integrate diverse inputs and coordinate a multitude of cellular behaviors. In this regard, Hippo signaling is a strong candidate in transducing external signals into organized cellular changes.

Supplementary Material

Refer to Web version on PubMed Central for supplementary material.

Acknowledgements

We thank members of the Chuang laboratory for helpful discussions, Ryan Guterres, Audrey Liu, Kuldeep Kumawat and Stacey Croll for technical assistance, Cheryl Chapin for reagents and Ross Metzger for critical reading of the manuscript. This work was supported by grants from the National Institutes of Health (U01 HL111054) to P.T. C.

References

Barry ER, Camargo FD. The Hippo superhighway: signaling crossroads converging on the Hippo/Yap pathway in stem cells and development. Current opinion in cell biology. 2013; 25:247–253. [PubMed: 23312716]

Borok Z, Whitsett JA, Bitterman PB, Thannickal VJ, Kotton DN, Reynolds SD, Krasnow MA, Bianchi DW, Morrisey EE, Hogan BL, Kurie JM, Walker DC, Radisky DC, Nishimura SL, Violette SM, Noble PW, Shapiro SD, Blaisdell CJ, Chapman HA, Kiley J, Gail D, Hoshizaki D. Cell plasticity in lung injury and repair: report from an NHLBI workshop, April 19-20, 2010. Proc Am Thorac Soc. 2011; 8:215–222. [PubMed: 21653526]

Chan EH, Nousiainen M, Chalamalasetty RB, Schafer A, Nigg EA, Sillje HH. The Ste20-like kinase Mst2 activates the human large tumor suppressor kinase Lats1. Oncogene. 2005; 24:2076–2086. [PubMed: 15688006]

Chan SW, Lim CJ, Chong YF, Pobbati AV, Huang C, Hong W. Hippo pathway-independent restriction of TAZ and YAP by angiomotin. The Journal of biological chemistry. 2011; 286:7018–7026. [PubMed: 21224387]

Chen MH, Wilson CW, Li YJ, Law KK, Lu CS, Gacayan R, Zhang X, Hui CC, Chuang PT. Cilium-independent regulation of Gli protein function by Sufu in Hedgehog signaling is evolutionarily conserved. Genes & development. 2009; 23:1910–1928. [PubMed: 19684112]

Chiang C, Litingtung Y, Lee E, Young KE, Corden JL, Westphal H, Beachy PA. Cyclopia and defective axial patterning in mice lacking Sonic hedgehog gene function. Nature. 1996; 383:407–413. [PubMed: 8837770]

Chung C, Kim T, Kim M, Kim M, Song H, Kim TS, Seo E, Lee SH, Kim H, Kim SK, Yoo G, Lee DH, Hwang DS, Kinashi T, Kim JM, Lim DS. Hippo-Foxa2 signaling pathway plays a role in peripheral lung maturation and surfactant homeostasis. Proceedings of the National Academy of Sciences of the United States of America. 2013; 110:7732–7737. [PubMed: 23620511]

Dobbs LG, Johnson MD, Vanderbilt J, Allen L, Gonzalez R. The great big alveolar TI cell: evolving concepts and paradigms. Cell Physiol Biochem. 2010; 25:55–62. [PubMed: 20054144]

Domyan ET, Sun X. Patterning and plasticity in development of the respiratory lineage. Developmental dynamics : an official publication of the American Association of Anatomists. 2011; 240:477–485. [PubMed: 21337460]

Gumbiner BM, Kim NG. The Hippo-YAP signaling pathway and contact inhibition of growth. Journal of cell science. 2014; 127:709–717. [PubMed: 24532814]

Halder G, Johnson RL. Hippo signaling: growth control and beyond. Development. 2011; 138:9–22. [PubMed: 21138973]

Hardie WD, Hagood JS, Dave V, Perl AK, Whitsett JA, Korfhagen TR, Glasser S. Signaling pathways in the epithelial origins of pulmonary fibrosis. Cell Cycle. 2010; 9:2769–2776. [PubMed: 20676040]

Harfe BD, Scherz PJ, Nissim S, Tian H, McMahon AP, Tabin CJ. Evidence for an expansion-based temporal Shh gradient in specifying vertebrate digit identities. Cell. 2004; 118:517–528. [PubMed: 15315763]

Harvey KF, Hariharan IK. The hippo pathway. Cold Spring Harbor perspectives in biology. 2012; 4:a011288. [PubMed: 22745287]

Herriges M, Morrisey EE. Lung development: orchestrating the generation and regeneration of a complex organ. Development. 2014; 141:502–513. [PubMed: 24449833]

Huang J, Wu S, Barrera J, Matthews K, Pan D. The Hippo signaling pathway coordinately regulates cell proliferation and apoptosis by inactivating Yorkie, the Drosophila Homolog of YAP. Cell. 2005; 122:421–434. [PubMed: 16096061]

Jacquemin P, Hwang JJ, Martial JA, Dolle P, Davidson I. A novel family of developmentally regulated mammalian transcription factors containing the TEA/ATTS DNA binding domain. The Journal of biological chemistry. 1996; 271:21775–21785. [PubMed: 8702974]

Katagiri K, Katakai T, Ebisuno Y, Ueda Y, Okada T, Kinashi T. Mst1 controls lymphocyte trafficking and interstitial motility within lymph nodes. The EMBO journal. 2009; 28:1319–1331. [PubMed: 19339990]

Kotton DN. Next-generation regeneration: the hope and hype of lung stem cell research. American journal of respiratory and critical care medicine. 2012; 185:1255–1260. [PubMed: 22517787]

Lieber M, Smith B, Szakal A, Nelson-Rees W, Todaro G. A continuous tumor-cell line from a human lung carcinoma with properties of type II alveolar epithelial cells. International journal of cancer. Journal international du cancer. 1976; 17:62–70. [PubMed: 175022]

Lin C, Song H, Huang C, Yao E, Gacayan R, Xu SM, Chuang PT. Alveolar type II cells possess the capability of initiating lung tumor development. PloS one. 2012; 7:e53817. [PubMed: 23285300]

Mahoney JE, Mori M, Szymaniak AD, Varelas X, Cardoso WV. The hippo pathway effector Yap controls patterning and differentiation of airway epithelial progenitors. Developmental cell. 2014; 30:137–150. [PubMed: 25043473]

Makita R, Uchijima Y, Nishiyama K, Amano T, Chen Q, Takeuchi T, Mitani A, Nagase T, Yatomi Y, Aburatani H, Nakagawa O, Small EV, Cobo-Stark P, Igarashi P, Murakami M, Tominaga J, Sato T, Asano T, Kurihara Y, Kurihara H. Multiple renal cysts, urinary concentration defects, and pulmonary emphysematous changes in mice lacking TAZ. American journal of physiology. Renal physiology. 2008; 294:F542–553. [PubMed: 18172001]

Matsui Y, Lai ZC. Mutual regulation between Hippo signaling and actin cytoskeleton. Protein & cell. 2013; 4:904–910. [PubMed: 24248471]

Morin-Kensicki EM, Boone BN, Howell M, Stonebraker JR, Teed J, Alb JG, Magnuson TR, O'Neal W, Milgram SL. Defects in yolk sac vasculogenesis, chorioallantoic fusion, and embryonic axis elongation in mice with targeted disruption of Yap65. Molecular and cellular biology. 2006; 26:77–87. [PubMed: 16354681]

Morrisey EE, Cardoso WV, Lane RH, Rabinovitch M, Abman SH, Ai X, Albertine KH, Bland RD, Chapman HA, Checkley W, Epstein JA, Kintner CR, Kumar M, Minoo P, Mariani TJ, McDonald DM, Mukouyama YS, Prince LS, Reese J, Rossant J, Shi W, Sun X, Werb Z, Whitsett JA, Gail D, Blaisdell CJ, Lin QS. Molecular determinants of lung development. Ann Am Thorac Soc. 2013; 10:S12–16. [PubMed: 23607856]

Oh S, Lee D, Kim T, Kim TS, Oh HJ, Hwang CY, Kong YY, Kwon KS, Lim DS. Crucial role for Mst1 and Mst2 kinases in early embryonic development of the mouse. Molecular and cellular biology. 2009; 29:6309–6320. [PubMed: 19786569]

Oka T, Mazack V, Sudol M. Mst2 and Lats kinases regulate apoptotic function of Yes kinase-associated protein (YAP). The Journal of biological chemistry. 2008; 283:27534–27546. [PubMed: 18640976]

Ornitz DM, Yin Y. Signaling networks regulating development of the lower respiratory tract. Cold Spring Harbor perspectives in biology. 2012; 4

Ota M, Sasaki H. Mammalian Tead proteins regulate cell proliferation and contact inhibition as transcriptional mediators of Hippo signaling. Development. 2008; 135:4059–4069. [PubMed: 19004856]

Pan D. The hippo signaling pathway in development and cancer. Developmental cell. 2010; 19:491–505. [PubMed: 20951342]

Rawlins EL, Perl AK. The a"MAZE"ing world of lung-specific transgenic mice. American journal of respiratory cell and molecular biology. 2012; 46:269–282. [PubMed: 22180870]

Reginensi A, Scott RP, Gregorieff A, Bagherie-Lachidan M, Chung C, Lim DS, Pawson T, Wrana J, McNeill H. Yap- and Cdc42-dependent nephrogenesis and morphogenesis during mouse kidney development. PLoS genetics. 2013; 9:e1003380. [PubMed: 23555292]

Reynolds A, Leake D, Boese Q, Scaringe S, Marshall WS, Khvorova A. Rational siRNA design for RNA interference. Nature biotechnology. 2004; 22:326–330.

Sawada A, Kiyonari H, Ukita K, Nishioka N, Imuta Y, Sasaki H. Redundant roles of Tead1 and Tead2 in notochord development and the regulation of cell proliferation and survival. Molecular and cellular biology. 2008; 28:3177–3189. [PubMed: 18332127]

Schlegelmilch K, Mohseni M, Kirak O, Pruszak J, Rodriguez JR, Zhou D, Kreger BT, Vasioukhin V, Avruch J, Brummelkamp TR, Camargo FD. Yap1 acts downstream of alpha-catenin to control epidermal proliferation. Cell. 2011; 144:782–795. [PubMed: 21376238]

Shi W, Chen F, Cardoso WV. Mechanisms of lung development: contribution to adult lung disease and relevance to chronic obstructive pulmonary disease. Proc Am Thorac Soc. 2009; 6:558–563. [PubMed: 19934349]

Song H, Mak KK, Topol L, Yun K, Hu J, Garrett L, Chen Y, Park O, Chang J, Simpson RM, Wang CY, Gao B, Jiang J, Yang Y. Mammalian Mst1 and Mst2 kinases play essential roles in organ size control and tumor suppression. Proceedings of the National Academy of Sciences of the United States of America. 2010; 107:1431–1436. [PubMed: 20080598]

Song H, Yao E, Lin C, Gacayan R, Chen MH, Chuang PT. Functional characterization of pulmonary neuroendocrine cells in lung development, injury, and tumorigenesis. Proceedings of the National Academy of Sciences of the United States of America. 2012; 109:17531–17536. [PubMed: 23047698]

Staley BK, Irvine KD. Hippo signaling in Drosophila: recent advances and insights. Developmental dynamics : an official publication of the American Association of Anatomists. 2012; 241:3–15. [PubMed: 22174083]

Sudol M. Yes-associated protein (YAP65) is a proline-rich phosphoprotein that binds to the SH3 domain of the Yes proto-oncogene product. Oncogene. 1994; 9:2145–2152. [PubMed: 8035999]

Sudol M, Bork P, Einbond A, Kastury K, Druck T, Negrini M, Huebner K, Lehman D. Characterization of the mammalian YAP (Yes-associated protein) gene and its role in defining a novel protein module, the WW domain. The Journal of biological chemistry. 1995; 270:14733–14741. [PubMed: 7782338]

Varelas X. The Hippo pathway effectors TAZ and YAP in development, homeostasis and disease. Development. 2014; 141:1614–1626. [PubMed: 24715453]

Wan H, Dingle S, Xu Y, Besnard V, Kaestner KH, Ang SL, Wert S, Stahlman MT, Whitsett JA. Compensatory roles of Foxa1 and Foxa2 during lung morphogenesis. The Journal of biological chemistry. 2005; 280:13809–13816. [PubMed: 15668254]

Wan H, Kaestner KH, Ang SL, Ikegami M, Finkelman FD, Stahlman MT, Fulkerson PC, Rothenberg ME, Whitsett JA. Foxa2 regulates alveolarization and goblet cell hyperplasia. Development. 2004; 131:953–964. [PubMed: 14757645]

Warburton D, El-Hashash A, Carraro G, Tiozzo C, Sala F, Rogers O, De Langhe S, Kemp PJ, Riccardi D, Torday J, Bellusci S, Shi W, Lubkin SR, Jesudason E. Lung organogenesis. Curr Top Dev Biol. 2010; 90:73–158. [PubMed: 20691848]

Wikenheiser KA, Vorbroker DK, Rice WR, Clark JC, Bachurski CJ, Oie HK, Whitsett JA. Production of immortalized distal respiratory epithelial cell lines from surfactant protein C/simian virus 40 large tumor antigen transgenic mice. Proceedings of the National Academy of Sciences of the United States of America. 1993; 90:11029–11033. [PubMed: 8248207]

Xin M, Kim Y, Sutherland LB, Murakami M, Qi X, McAnally J, Porrello ER, Mahmoud AI, Tan W, Shelton JM, Richardson JA, Sadek HA, Bassel-Duby R, Olson EN. Hippo pathway effector Yap promotes cardiac regeneration. Proceedings of the National Academy of Sciences of the United States of America. 2013; 110:13839–13844. [PubMed: 23918388]

Xin M, Kim Y, Sutherland LB, Qi X, McAnally J, Schwartz RJ, Richardson JA, Bassel-Duby R, Olson EN. Regulation of insulin-like growth factor signaling by Yap governs cardiomyocyte proliferation and embryonic heart size. Science signaling. 2011; 4:ra70. [PubMed: 22028467]

Xu Q, Tam M, Anderson SA. Fate mapping Nkx2.1-lineage cells in the mouse telencephalon. The Journal of comparative neurology. 2008; 506:16–29. [PubMed: 17990269]

Yu FX, Guan KL. The Hippo pathway: regulators and regulations. Genes & development. 2013; 27:355–371. [PubMed: 23431053]

Zhang H, Liu CY, Zha ZY, Zhao B, Yao J, Zhao S, Xiong Y, Lei QY, Guan KL. TEAD transcription factors mediate the function of TAZ in cell growth and epithelialmesenchymal transition. The Journal of biological chemistry. 2009; 284:13355–13362. [PubMed: 19324877]

Zhang N, Bai H, David KK, Dong J, Zheng Y, Cai J, Giovannini M, Liu P, Anders RA, Pan D. The Merlin/NF2 tumor suppressor functions through the YAP oncoprotein to regulate tissue homeostasis in mammals. Developmental cell. 2010; 19:27–38. [PubMed: 20643348]

Zhao B, Li L, Tumaneng K, Wang CY, Guan KL. A coordinated phosphorylation by Lats and CK1 regulates YAP stability through SCF(beta-TRCP). Genes & development. 2010; 24:72–85. [PubMed: 20048001]

Zhao B, Wei X, Li W, Udan RS, Yang Q, Kim J, Xie J, Ikenoue T, Yu J, Li L, Zheng P, Ye K, Chinnaiyan A, Halder G, Lai ZC, Guan KL. Inactivation of YAP oncoprotein by the Hippo pathway is involved in cell contact inhibition and tissue growth control. Genes & development. 2007; 21:2747–2761. [PubMed: 17974916]

Zhao B, Ye X, Yu J, Li L, Li W, Li S, Yu J, Lin JD, Wang CY, Chinnaiyan AM, Lai ZC, Guan KL. TEAD mediates YAP-dependent gene induction and growth control. Genes & development. 2008; 22:1962–1971. [PubMed: 18579750]

Zhao R, Fallon TR, Saladi SV, Pardo-Saganta A, Villoria J, Mou H, Vinarsky V, Gonzalez-Celeiro M, Nunna N, Hariri LP, Camargo F, Ellisen LW, Rajagopal J. Yap tunes airway epithelial size and architecture by regulating the identity, maintenance, and self-renewal of stem cells. Developmental cell. 2014; 30:151–165. [PubMed: 25043474]

Zhou D, Conrad C, Xia F, Park JS, Payer B, Yin Y, Lauwers GY, Thasler W, Lee JT, Avruch J, Bardeesy N. Mst1 and Mst2 maintain hepatocyte quiescence and suppress hepatocellular carcinoma development through inactivation of the Yap1 oncogene. Cancer cell. 2009; 16:425–438. [PubMed: 19878874]

Highlights

- Loss of *Mst1/2* in the mouse lung epithelium leads to neonatal lethality
- Lung cell type specification is disrupted in the absence of *Mst1/2*
- Expression of YAP targets is elevated in *Mst1/2* mutant lungs
- Genetic removal of one copy of *Yap* rescues lung phenotypes in *Mst1/2* mutants
- A conserved MST1/2-YAP axis controls lung growth during development

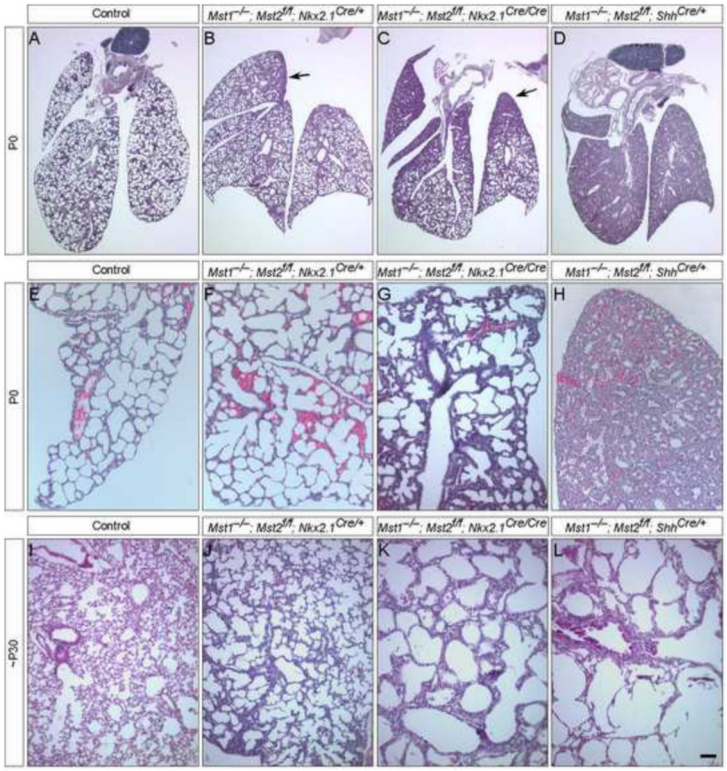

Figure 1.

Histological analysis of *Mst1/2*-deficient lungs generated by different mouse Cre lines (A-L) Hematoxylin-and-eosin (H&E)-stained lung sections collected from mouse strains that carry various combinations of $Mst1^{-}$ (null), $Mst2^{f}$ (conditional) and *Cre* alleles. (A-D) At postnatal (p) day 0 (P0), lungs from $Mst1^{-/-}; Mst2^{f/f}; Shh^{Cre/+}$ mice did not expand and appeared dense and compact compared to lungs from their wild-type littermates. By contrast, lungs from either $Mst1^{-/-}; Mst2^{f/f}; Nkx2.1^{Cre/+}$ or $Mst1^{-/-}; Mst2^{f/f}; Nkx2.1^{Cre/Cre}$ mice were inflated although the upper regions of the lobes (arrows) were more compressed and contained less air. (E-H) Extra lung cells were detected in $Mst1^{-/-}; Mst2^{f/f}; Nkx2.1^{Cre/+}$, $Mst1^{-/-}; Mst2^{f/f}; Nkx2.1^{Cre/Cre}$ and $Mst1^{-/-}; Mst2^{f/f}; Shh^{Cre/+}$ lungs and the severity of the lung phenotype increased in that order. While most $Mst1^{-/-}; Mst2^{f/f}; Shh^{Cre/+}$ mice died soon after birth, both $Mst1^{-/-}; Mst2^{f/f}; Nkx2.1^{Cre/+}$ and $Mst1^{-/-}; Mst2^{f/f}; Nkx2.1^{Cre/Cre}$ mice survived postnatally. (I-L) Lungs from $Mst1^{-/-}; Mst2^{f/f}; Nkx2.1^{Cre/Cre}$ mice at various time points after birth showed morphological abnormalities, including extra lung cells and inflammatory responses. In some $Mst1^{-/-}; Mst2^{f/f}; Nkx2.1^{Cre/Cre}$ animals, collapsed lung lobes could be observed, likely due to ongoing destruction of the lungs. Rare $Mst1^{-/-}; Mst2^{f/f}; Shh^{Cre/+}$ mice escaped neonatal lethality and some of them displayed varying degrees of lung defects. Scale bar = 500 μm for A-D; 100 μm for E-L.

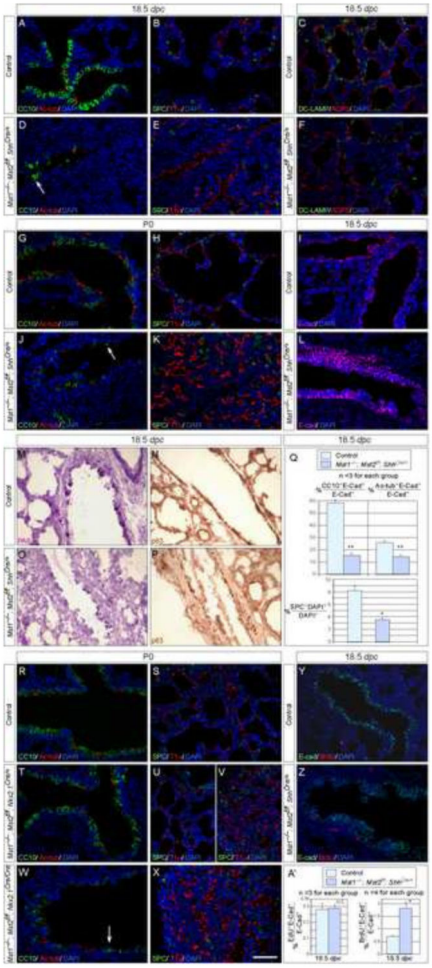

Figure 2.

Phenotypic analysis of *Mst1/2* mutant lungs produced by different mouse Cre lines (A-P) Immunostaining of lung sections collected from mouse strains that carry various combinations of *Mst1*$^{-}$ (null), *Mst2*^{f} (conditional) and Cre alleles at 18.5 *dpc* or postnatal day 0 (P0). (A-L) Major lung cell types including Clara cells (CC10^{+}), ciliated cells (Ac-tubulin^{+}), alveolar type II cells (SPC^{+}, DC-LAMP^{+}) and alveolar type I cells (T1α^{+}, AQP5^{+}) were specified in *Mst1*$^{-/-}$*; Mst2*$^{f/f}$*; Shh*$^{Cre/+}$ lungs at 18.5 *dpc* or P0. However, fewer CC10^{+} and Ac-tubulin^{+} cells in the conducting airways (arrows) and fewer type II cells in the alveoli were detected in *Mst1*$^{-/-}$*; Mst2*$^{f/f}$*; Shh*^{Cre} compared to control lungs. Quantification of cell numbers is shown in (Q) in which the percentage of epithelial cells (E-cadherin^{+} [E-cad^{+}]) that express CC10 or Ac-tubulin was calculated; the percentage of SPC^{+} cells on lung sections was enumerated by counting the total number of cells using DAPI. In many bronchioles, the simple columnar epithelium in wild-type lungs (I) is replaced by pseudostratified epithelium (L) in *Mst1/2*-deficient lungs. Note that A–B and D–E are adjacent sections. (M-P) Immunohistochemistry of lung sections for detecting PAS^{+} mucin-secreting goblet cells and p63^{+} basal cells. Both cell types can be readily detected in *Mst1*$^{-/-}$*; Mst2*$^{f/f}$*; Shh*$^{Cre/+}$ lungs at 18.5 *dpc*. (R-X) Major lung cell types were also present in *Mst1*$^{-/-}$*; Mst2*$^{f/f}$*; Nkx2.1*$^{Cre/+}$ and *Mst1*$^{-/-}$*; Mst2*$^{f/f}$*; Nkx2.1*$^{Cre/Cre}$ lungs at P0. Similarly,

the number of $CC10^+$ and Ac-tubulin$^+$ cells in the conducting airways (arrow) was reduced in *Mst1*$^{-/-}$*; Mst2*$^{f/f}$*; Nkx2.1*$^{Cre/Cre}$ lungs compared to control lungs. Image in (U) was taken from the lower lobe and (V) from the upper lobe of *Mst1*$^{-/-}$*; Mst2*$^{f/f}$*; Nkx2.1*$^{Cre/+}$ lungs. (Y, Z) Immunostaining of lung sections collected from *Mst1*$^{-/-}$*; Mst2*$^{f/f}$*; Shh*$^{Cre/+}$ mice injected with BrdU or EdU. Lung epithelial cells were distinguished by E-cad staining. Cell proliferation rate (judged by BrdU or EdU staining) in the lung epithelium was quantified in (A'). While the number of BrdU$^+$ or EdU$^+$ cells was increased in the epithelium of *Mst1*$^{-/-}$*; Mst2*$^{f/f}$*; Shh*$^{Cre/+}$ lungs at 18.5 *dpc*, no apparent difference in the number of epithelial EdU$^+$ cells was detected between control and *Mst1*$^{-/-}$*; Mst2*$^{f/f}$*; Shh*$^{Cre/+}$ lungs at 16.5 *dpc*. This is correlated with the lack of overt lung phenotypes in *Mst1*$^{-/-}$*; Mst2*$^{f/f}$*; Shh*$^{Cre/+}$ mice at 16.5 *dpc*. It is possible that increased cell proliferation and phenotypic consequences only become apparent after 16.5 *dpc*. Scale bar = 50 μm. * $P < 0.05$; ** $P < 0.01$; NS, not significant (unpaired Student's *t*-test).

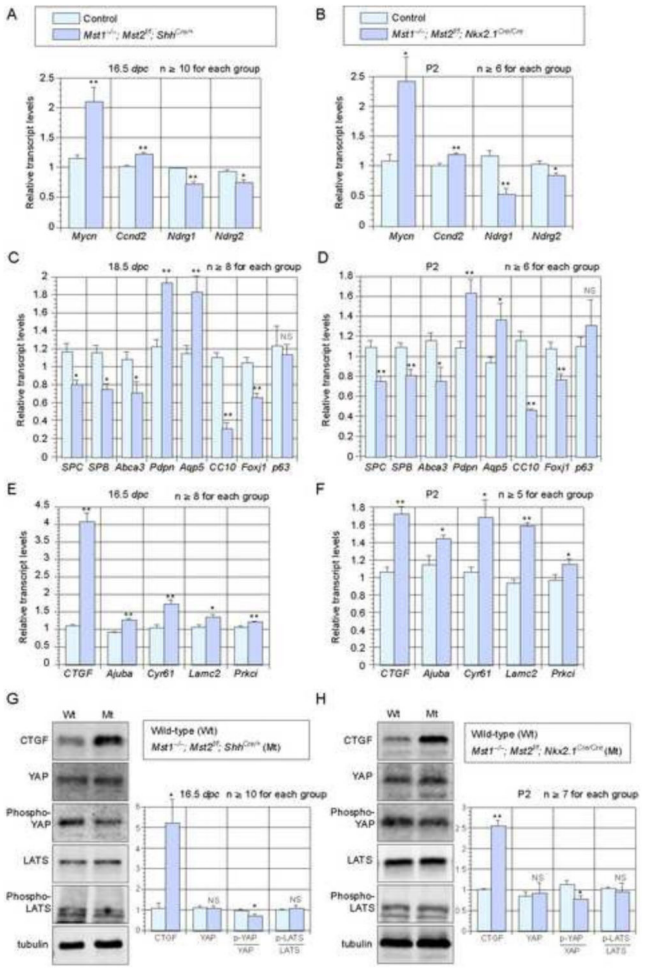

Figure 3.

Molecular analysis of lung cell type markers, cell cycle regulators, YAP targets and YAP/LATS proteins in the absence of *Mst1/2* in the lung

(A-F) qPCR analysis of RNA extracted from *Mst1*$^{-/-}$*; Mst2*$^{f/f}$*; Shh*$^{Cre/+}$ (16.5 or 18.5 *dpc*) and *Mst1*$^{-/-}$*; Mst2*$^{f/f}$*; Nkx2.1*$^{Cre/Cre}$ (P2) lungs. (A, B) Expression of several cell cycle regulators (*Mycn* and *Ccnd2*) and MYCN targets (*Ndrg1* and *Ndrg2*) was increased in both *Mst1*$^{-/-}$*; Mst2*$^{f/f}$*; Shh*$^{Cre/+}$ and *Mst1*$^{-/-}$*; Mst2*$^{f/f}$*; Nkx2.1*$^{Cre/Cre}$ lungs. (C, D) Alterations in expression of various lung cell markers followed a similar trend in *Mst1*$^{-/-}$*; Mst2*$^{f/f}$*; Shh*$^{Cre/+}$ and *Mst1*$^{-/-}$*; Mst2*$^{f/f}$*; Nkx2.1*$^{Cre/Cre}$ lungs. While expression of alveolar type II cell markers (*SPC*, *SPB*, *Abca3*), Clara cell marker (*CC10*), ciliated cell marker (*Foxj1*) was reduced, expression of alveolar type I markers (*Pdpn*, *Aqp5*) was elevated. Basal cell marker (*p63*) did not seem to be altered. (E, F) Expression of YAP targets (*Ctgf*, *Ajuba*, *Cyr61*, *Lamc2* and *Prkci*) was significantly induced in both *Mst1*$^{-/-}$*; Mst2*$^{f/f}$*; Shh*$^{Cre/+}$ and *Mst1*$^{-/-}$*; Mst2*$^{f/f}$*; Nkx2.1*$^{Cre/Cre}$ lungs albeit *Ctgf* induction was more modest in *Mst1*$^{-/-}$*; Mst2*$^{f/f}$*; Nkx2.1*$^{Cre/Cre}$ lungs. (G, H) Western blot analysis of YAP and phospho-YAP protein levels using lysates derived from *Mst1*$^{-/-}$*; Mst2*$^{f/f}$*; Shh*$^{Cre/+}$ and *Mst1*$^{-/-}$*; Mst2*$^{f/f}$*; Nkx2.1*$^{Cre/Cre}$ lungs at 16.5 *dpc* and P2 respectively. The fraction of phospho-YAP protein (relative to the total YAP) was decreased in *Mst1*$^{-/-}$*; Mst2*$^{f/f}$*; Shh*$^{Cre/+}$ or *Mst1*$^{-/-}$*; Mst2*$^{f/f}$*; Nkx2.1*$^{Cre/Cre}$

lungs. By contrast, protein levels of LATS and phospho-LATS did not seem to be altered in *Mst1*$^{-/-}$*; Mst2*$^{f/f}$*; Shh*$^{Cre/+}$ or *Mst1*$^{-/-}$*; Mst2*$^{f/f}$*; Nkx2.1*$^{Cre/Cre}$ lungs. Tubulin was used as the loading control. All values are means ± SEM. * $P < 0.05$; ** $P < 0.01$; NS, not significant (unpaired Student's *t*-test).

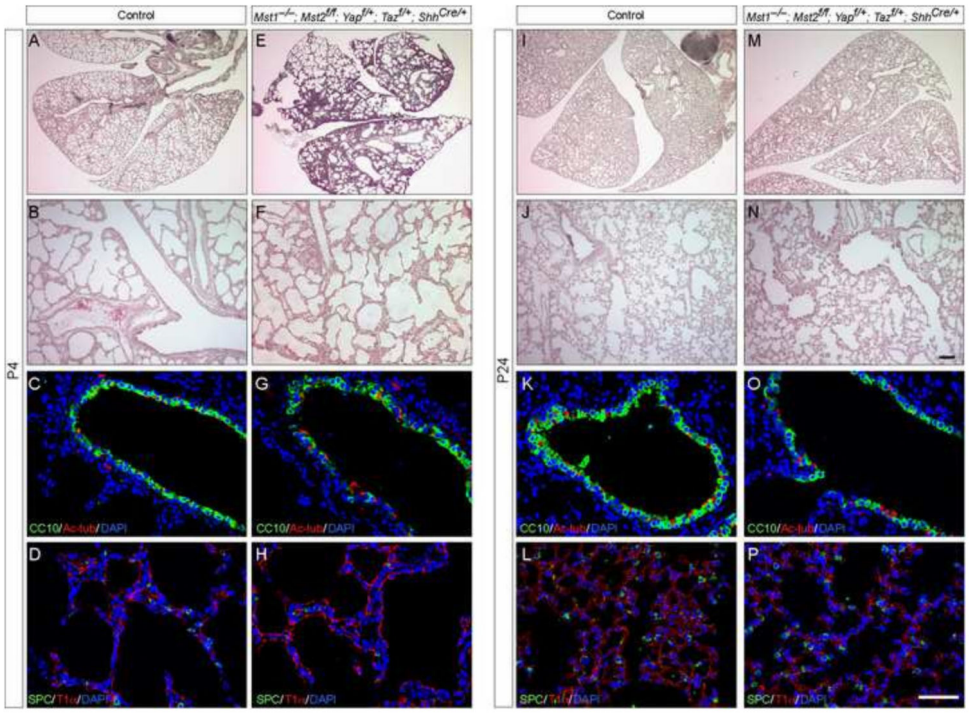

Figure 4.

The effects of *Yap/Taz* removal on the development of *Mst1/2* mutant lungs and the survival of the animals

(A, B, E, F, I, J, M, N) Hematoxylin-and-eosin (H&E)-stained lung sections collected from control and $Mst1^{-/-}; Mst2^{f/f}; Yap^{f/+}; Taz^{f/+}; Shh^{Cre/+}$ mice postnatal (p) day 4 (P4) and 24 (P24). Unlike $Mst1^{-/-}; Mst2^{f/f}; Shh^{Cre/+}$ mice, most of which died soon after birth, $Mst1^{-/-}; Mst2^{f/f}; Yap^{f/+}; Taz^{f/+}; Shh^{Cre/+}$ mice survived to adulthood without apparent gross abnormalities. In addition, lungs from $Mst1^{-/-}; Mst2^{f/f}; Yap^{f/+}; Taz^{f/+}; Shh^{Cre/+}$ mice were fully expanded and devoid of any dense or compact architecture observed in $Mst1^{-/-}; Mst2^{f/f}; Shh^{Cre/+}$ lungs. Lung histology was indistinguishable between control and $Mst1^{-/-}; Mst2^{f/f}; Yap^{f/+}; Taz^{f/+}; Shh^{Cre/+}$ mice (n > 20 analyzed). Note that some blood was present on lung sections (E) of $Mst1^{-/-}; Mst2^{f/f}; Yap^{f/+}; Taz^{f/+}; Shh^{Cre/+}$ mice due to dissection. (C, D, G, H, K, L, O, P) Immunostaining of lung sections collected from control and $Mst1^{-/-}; Mst2^{f/f}; Yap^{f/+}; Taz^{f/+}; Shh^{Cre/+}$ mice at P4 and P24. Lung cell types appeared to be properly specified in $Mst1^{-/-}; Mst2^{f/f}; Yap^{f/+}; Taz^{f/+}; Shh^{Cre/+}$ mice. Scale bar = 100 μm for A, B, E, F, I, J, M, N; 50 μm for C, D, G, H, K, L, O, P.

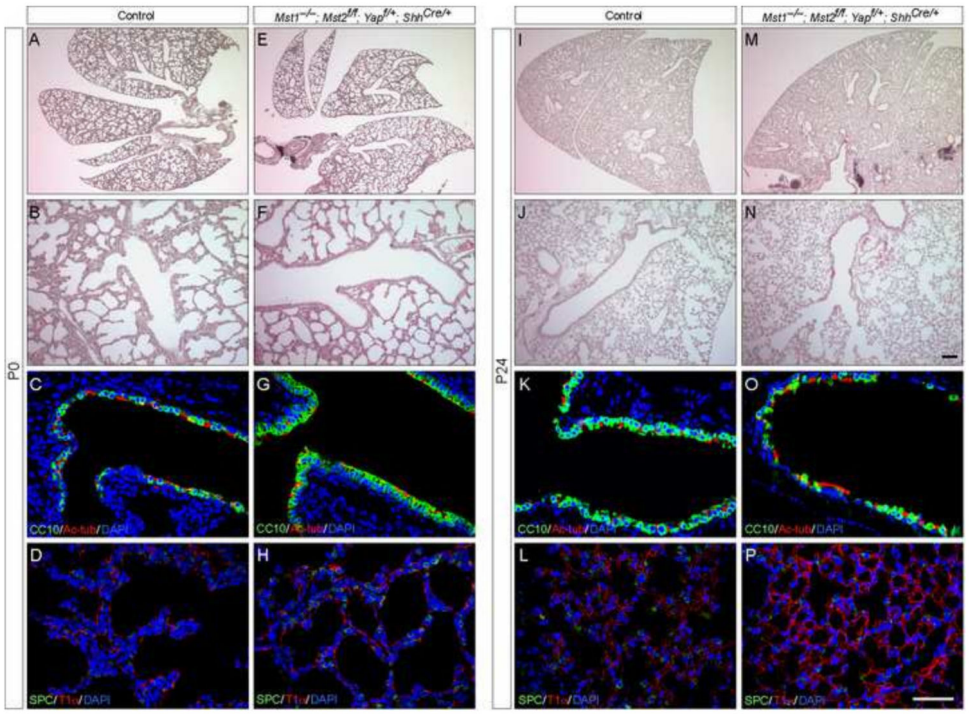

Figure 5.

The effects of *Yap* removal on the development of *Mst1/2* mutant lungs and the survival of the animals

(A, B, E, F, I, J, M, N) Hematoxylin-and-eosin (H&E)-stained lung sections collected from control and $Mst1^{-/-}; Mst2^{f/f}; Yap^{f/+}; Shh^{Cre/+}$ mice at postnatal (p) day 4 (P4) and 24 (P24). Unlike $Mst1^{-/-}; Mst2^{f/f}; Shh^{Cre/+}$ mice, most of which died soon after birth, $Mst1^{-/-}; Mst2^{f/f}; Yap^{f/+}; Shh^{Cre/+}$ mice survived to adulthood without apparent gross abnormalities. In addition, lungs from $Mst1^{-/-}; Mst2^{f/f}; Yap^{f/+}; Shh^{Cre/+}$ mice were fully expanded and devoid of any dense or compact architecture seen in $Mst1^{-/-}; Mst2^{f/f}; Shh^{Cre/+}$ lungs. Lung histology was indistinguishable between control and $Mst1^{-/-}; Mst2^{f/f}; Yap^{f/+}; Shh^{Cre/+}$ mice ($n > 8$ analyzed). (C, D, G, H, K, L, O, P) Immunostaining of lung sections collected from control and $Mst1^{-/-}; Mst2^{f/f}; Yap^{f/+}; Shh^{Cre/+}$ mice at P4 and P24. Lung cell types appeared to be properly specified in $Mst1^{-/-}; Mst2^{f/f}; Yap^{f/+}; Shh^{Cre/+}$ mice. Scale bar = 100 μm for A, B, E, F, I, J, M, N; 50 μm for C, D, G, H, K, L, O, P.

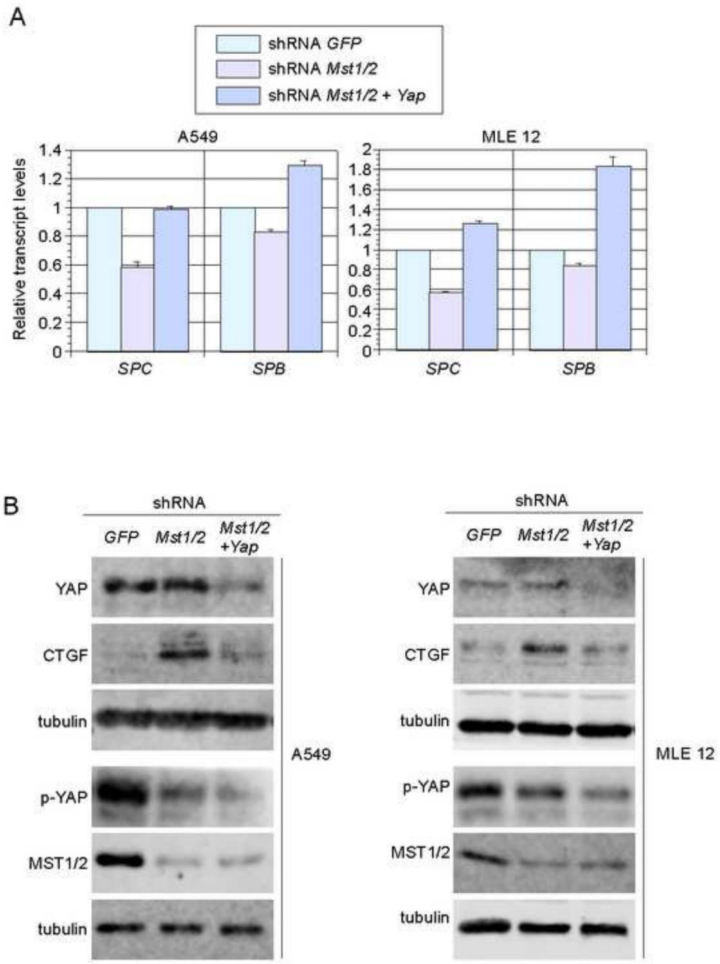

Figure 6.

The effects of *Mst1/2* and *Yap* knockdown on alveolar marker expression in lung cell lines (A, B) qPCR analysis of mRNA transcripts and Western blot analysis of proteins extracted from human A549 or mouse MLE 12 lung cell lines. In these studies, *Mst1/2* were knocked down individually or in combination with *Yap* inactivation by shRNA as indicated. shRNA against *GFP* served as a control. Knockdown of *Mst1/2* resulted in reduced expression of *SPB/SPC* (alveolar type II cell markers), consistent with findings in *Mst1/2*-deficient lungs. Inactivation of *Mst1/2* also led to increased CTGF (YAP target) expression and reduced levels of phospho-YAP, both of which are associated with increased YAP activity. Such alteration in gene expression was restored when *Yap* was simultaneously knocked down by shRNA in conjunction with *Mst1/2*. These results further support conclusions from analysis of *Mst1/2* mutant lungs. Tubulin was used as the loading control.

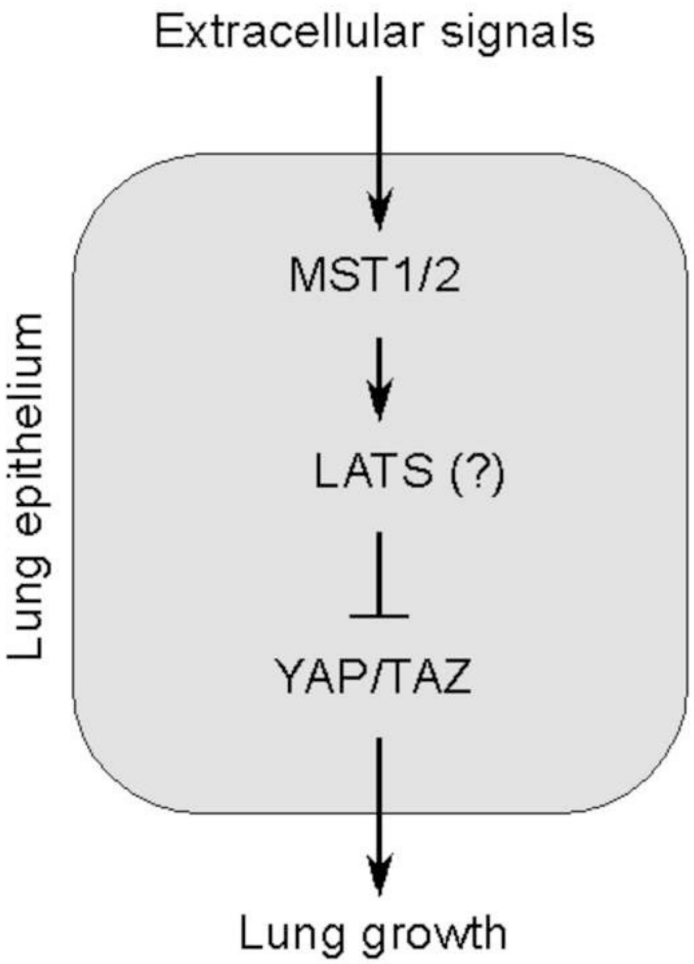

Figure 7.

A model of a conserved MST1/2-YAP axis in regulating lung development A model of MST and YAP interactions in the lung. Control of YAP/TAZ activity by MST1/2 regulates many aspects of cellular behavior during lung development. YAP plays a more dominant role than TAZ in Hippo signaling. In this model, loss of MST1/2 shifts YAP toward the non-phosphorylated state, which is no longer sequestered in the cytoplasm and also free from degradation. Instead, non-phosphorylated YAP is enriched in the nucleus to activate YAP targets, leading to cell proliferation and fate determination and other changes in cellular properties. This canonical relationship between MST and YAP is observed in many tissues. The mediator of Hippo signaling between MST1/2 and YAP in the lung could be LATS (another conserved feature of the Hippo pathway) or some other unknown kinases. Factors that activate MST1/2 have been inferred from cell-based studies but signals that control MST activity in the lung remain unclear.